Absorption Measurements Demonstrating the Importance of $\Delta n = 0$ Transitions in the Opacity of Iron

L. B. Da Silva,[1,2] B. J. MacGowan,[1] D. R. Kania,[1] B. A. Hammel,[1] C. A. Back,[1] E. Hsieh,[1] R. Doyas,[1] C. A. Iglesias,[1] F. J. Rogers,[1] and R. W. Lee[1]

[1]*Lawrence Livermore National Laboratory, P. O. Box 808, Livermore, California 94550*

[2]*Physics Department, University of California Berkeley, Berkeley, California 94720*

(Received 27 March 1992)

Novel opacity calculations, which treat in detail the spectra of medium-Z ions [Rogers and Iglesias, Astrophys. J. Suppl. Ser. **79**, 507 (1992)], produce results that are substantially different from opacity calculations extant in the literature. These new opacities provide solutions to a number of outstanding problems in astrophysics, thus providing an indirect validation of the theory. We report the results of an experiment measuring the photoabsorption in the spectral region from 50 to 120 eV of x-ray-heated iron which corroborate these new opacity calculations.

PACS numbers: 52.25.Nr, 44.40.+a, 52.50.Jm, 97.10.Ex

The study of spectra from ions with vacancies in the M shell and particularly the study of $\Delta n = 0$ transitions present a challenge due to the myriad transitions in the spectrum [1,2]. It has recently been shown that these transitions must be included in opacity calculations to obtain consistent stellar model predictions [3]. In general, the accuracy of opacity data is of central importance when radiation transfer is involved in determining the state of laboratory and astrophysical plasmas. Although opacity models have been of concern for a number of years [4], it was considered doubtful that possible errors in the atomic physics could affect the photon absorption cross sections to a degree large enough to make a substantial difference in the Rosseland mean opacity. In fact, the conventional wisdom was that the available opacity models, which were largely due to the long-term efforts of researchers at Los Alamos [5], were accurate to better than 25% over a wide range of temperature and density but never worse than 50% [6]. These calculations were performed within the constraints of the computational limits existing in the 1970s which required the use of hydrogenic formulas and scaling of photoionization cross sections. The increase in experimental accuracy led over the years to a number of astrophysical discrepancies between models using these opacities and observations. However, the changes in the opacity necessary to resolve some of these discrepancies are greater than factors of 3 and well beyond the stated accuracy [3,4,7]. In addition, there are numerous uncertainties in laboratory plasmas involving elements with low or moderate atomic number [8].

Recently a new opacity model, OPAL [9], has been developed which includes several improvements over the Los Alamos models. First, the atomic level structure is treated in detail in either $\mathcal{LS}$ or full intermediate coupling [10]. Second, and somewhat more subtle but of central importance to the generation of opacity, the equation of state—or equivalently the ensemble of level populations—is calculated self-consistently taking into account the plasma environment.

In previous opacity calculations a hybrid scheme was used for the atomic physics where the energy levels are in nl (e.g., $3s, 3p, \ldots$) and the oscillator strengths, f, are approximated as hydrogenic. The transmission through an iron plasma at a temperature of 25 eV and a density of 0.008 g/cm^3 (areal density of 2.0×10^{-5} g/cm^2) is presented in Fig. 1(a) for the hybrid scheme. The change in the opacity due to replacing hydrogenic with nonhy-

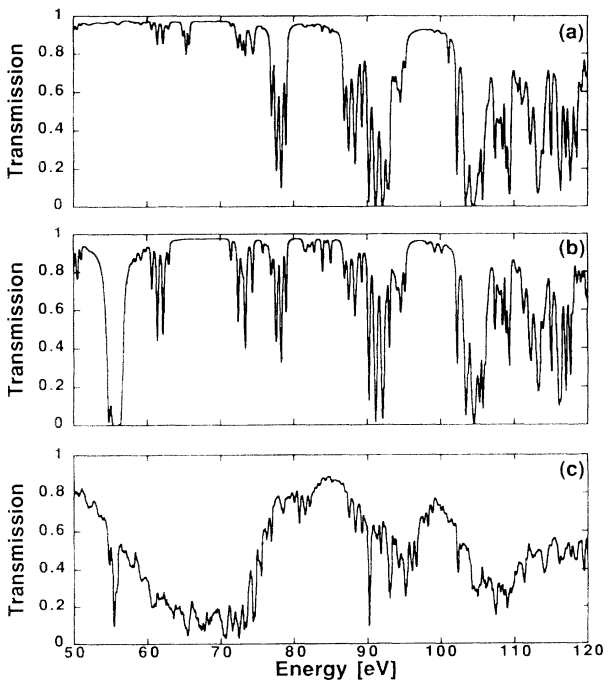

FIG. 1. Transmission calculations for an iron plasma with electron temperature of 25 eV and density of 8.0×10^{-3} g/cm^3 (areal density of 2.0×10^{-5} g/cm^2). (a) The hybrid scheme with hydrogenic f, (b) with nonhydrogenic f, and (c) full intermediate coupling. The total oscillator strengths for calculations (b) and (c) are equal.

drogenic f values is shown in Fig. 1(b). The most significant changes are the $n=3$ to 3 transitions at ~ 55 eV, which are absent from the opacity in Fig. 1(a). Note that this level of improvement makes no substantial difference in the Rosseland mean opacity, κ_R, which is a measure of photon absorption effects on the radiation flow [11]. This type of analysis could lead one to assume that the $\Delta n=0$ transitions and, therefore, configuration term structure are not necessary for the calculation of κ_R.

In Fig. 1(c) calculations with term splitting using intermediate coupling are shown. It can be seen that the effect of the term splitting is to produce a broad $\Delta n=0$ feature. For these plasma conditions the average number of bound electrons is ~ 18.5. This leads to complex spectra and an increase in the number of spectral lines of more than 2 orders of magnitude over the calculations in Fig. 1(a) or 1(b). Since κ_R preferentially weights the low photon absorption regions the broadening of the $\Delta n=0$ feature gives rise to a dramatic increase in κ_R. For the plasma conditions shown in Fig. 1, the κ_R for Fe using intermediate coupling is an order of magnitude larger than the other calculations.

This enhancement in the opacity has made significant impact on several astrophysical problems (e.g., pulsation properties of Cepheids [3], convective core overshooting [12], and solar models [13]). However, there is no direct confirmation of the theoretical model used to generate the opacity. The experiences of the past and the successes of the Rogers and Iglesias opacity calculations [9] indicate that it is essential to validate the new opacity theory by experiment. Consequently, we have focused on that feature which is the single most important modification of the iron opacity, that is, the $n=3$ to 3 transitions.

The methodology of the experiments uses a variation of the techniques developed to perform opacity measurements at the Nova laser [14]. A schematic drawing of the experiment is shown in Fig. 2. One laser beam with a wavelength of 0.53 μm is used to heat a 2500-Å Au foil by direct irradiation with a square 1-ns pulse of 3.3 kJ. A random phase plate and steering wedges were used to produce a nearly flat-topped and smooth intensity distribution over a 700-μm-diam focal spot. The x-ray flux which emerges from the back of the Au foil impinges on a sample consisting of 1000 Å CH on either side of a 200-Å layer of Fe. The angle, time, and frequency dependence of the x-ray flux from the back side of the Au foil has been previously measured and is thus known [15]. A radiation hydrodynamics simulation is used to calculate the temperature and density history of the sample in response to the measured x-ray flux and the results are plotted in Fig. 3. The curves represent the middle of the iron sample, and due to the CH tamping, the gradient in the sample is less than 5% in temperature and 10% in density. Thus x rays flood the sample and heat it to ~ 35 eV at densities ≥ 0.001 g/cm^3. These conditions are corroborated by previous measurements [15] of the ionization balance in the plasma as determined by absorption spectroscopy in the range between 100 and 200 eV. These plasma conditions are in the regime where the $n=3$ to 3 features of iron are predicted to be of major importance.

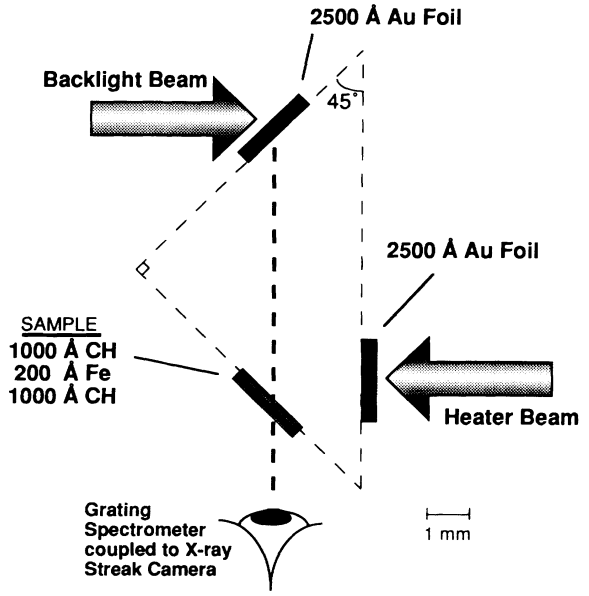

FIG. 2. A schematic drawing of the experimental setup. A laser beam irradiates a thin gold foil and produces x rays which heat the sample to be studied. Another laser beam irradiates a second gold foil over a variable 2-ns interval producing x rays which propagate through the sample and are recorded by a time-resolved grating spectrometer.

A second laser beam with a 2-ns square pulse of 0.53 μm light, which can be arbitrarily delayed in time, irradiates another 2500-Å Au foil. The beam is focused to a

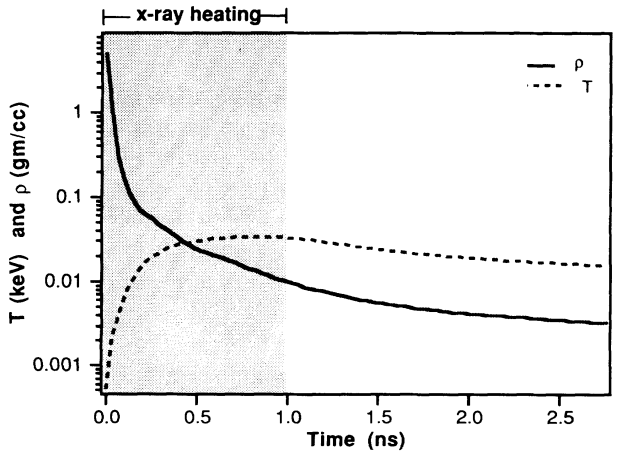

FIG. 3. Simulation of the sample under the influence of the measured x-ray flux from the heater. The temperature and the density are shown for the middle of the Fe sample vs time. The shaded region indicates the duration of the primary optical laser pulse.

300-μm-diam focal spot on the second Au foil which is aligned on the axis formed by the spectrometer and the sample. This x-ray source, which is 10 times further away from the sample than the heater, is the absorption probe (or backlighter) whose transmission through the sample is time resolved with the spectrometer. The following measurements have been performed to ensure the integrity of the sample [15]. (1) Stray laser light impinging on the Fe sample was measured to be less than 10^8 W/cm^2 and consequently has negligible effect on the sample. (2) The sample is uniformly heated by the x rays. (3) The expansion of a sample under x-ray heating was independently measured and found to be in agreement with hydrodynamic simulations. Note that the x rays heat the sample uniformly and therefore the radiation hydrodynamics are simpler than in cases where a laser impinges directly on a target.

The primary diagnostic instrument is a time-resolved x-ray UV spectrometer utilizing a Harada 1200-lines/mm varied line space grating manufactured by Hitachi [16] with an x-ray streak camera as the detector. An iridium-coated relay mirror positioned between the grating and streak camera discriminates against short-wavelength x rays which could appear in higher orders. The Harada grating has high efficiency at high order [17] and significant effort was put into rejecting these contributions in order to obtain a pure absorption spectrum. The combination of the Ir mirror at 11° to 16° grazing angle of incidence, and a 1300-Å Al filter resulted in the elimination of higher-order signals. For example, at 78 eV the rejection is 140:1 for second order (156-eV x rays) and 500:1 for third order (234-eV x rays), while at 72 eV the rejection is 1000:1 for second order and 4500:1 for third order.

Continuous time resolution is provided by using an x-ray streak camera with a CsI photocathode and measured time resolution of 30 ps. The streak camera has a fiber optic timing fiducial that allows the recorded spectra to be referenced to the laser beams and other diagnostics to $\sim$30 ps precision [18]. This timing marker allowed us to reference the time history of the absorption spectrum with the time history of the x-ray heating plasma.

The experiments performed consisted of several laser shots using various laser and sample configurations. The measurements made were the following: (1) cold Fe tests using a backlighter only to measure the effect of the backlighter on the sample; (2) CH absorption using a pure CH sample (2000 Å), a heating x-ray flux and a backlighter to provide absorption spectra; (3) Fe absorption using an Fe sample (1000 Å CH–200 Å Fe–1000 Å CH), a heating x-ray flux, and a backlighter to provide absorption spectra; (4) CH emissivity using the CH sample with heating x-ray flux only; and (5) Fe emissivity using an Fe sample with heating x-ray flux only. In all these measurements the spectrometer was apertured to observe only the central 500-μm-diam region of the foil. This ensured we were probing a uniform region of the sample.

The summary of the results is as follows. The cold Fe (1) test showed a clear cold Fe opacity with some insignificant warming 2.0 ns after the start of the backlighter pulse. The CH and Fe opacity experiments [(2) and (3)] show clear absorption spectra from heated matter while the emissivity experiments [(4) and (5)] showed no absorption features. The data were analyzed by first converting from film density to intensity using a calibrated step wedge. The emissivities of the CH and Fe sample are determined and subtracted from the CH and Fe absorption experiments, respectively. The results are then divided, which removes the x-ray energy dependence of the detector sensitivity, to yield the transmission through the Fe only. The unprocessed emissivity and absorption spectra at time 1.9 ns after the initiation of the heater pulse for the Fe sample are shown in Fig. 4(a). These spectra along with the analog CH sample spectra were used to determine the Fe transmission shown in Fig. 4(b). The error in the transmission curve is estimated to be ± 0.1 and is primarily due to small ($\pm 5\%$) variations in backlighter x-ray intensity as deduced from a spectrograph monitoring the backlighter plasma emission.

The measured Fe transmission is in reasonable agreement with the OPAL calculations shown in Fig. 1(c). The dominant feature centered at 70 eV is in good agreement with the expected position of the $\Delta n = 0$ (3-3) absorption peak. It is important to note that the Fe emissivity which we calculate by subtracting the CH emissivity from the data and removing the instrument response also shows a strong emission feature in this energy range. This is further support for the importance of the $\Delta n = 0$ transitions. Note that previous opacity models which

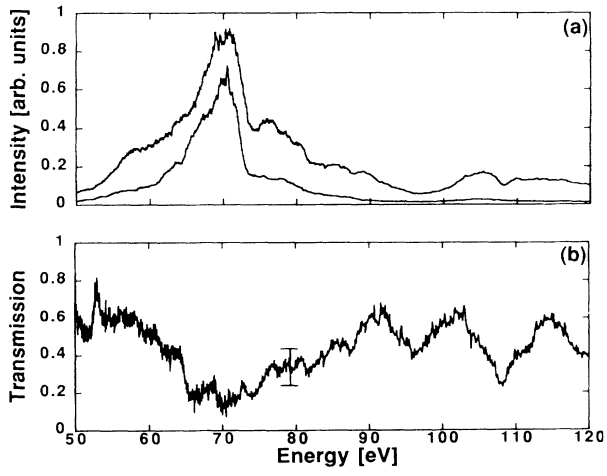

FIG. 4. (a) The measured x-ray spectrum for a tamped Fe sample with (upper) and without (lower) backlighter beam at a time 1.9 ns after the start of the heater pulse. (b) The experimentally measured transmission at the same instant in time.

neglected term splitting predict no large absorption feature in the energy range from 60 to 90 eV [Figs. 1(a) and 1(b)]. The $\Delta n = 1$ features predicted by OPAL to be around 93 and 107 eV are also observed in the measured transmission. It is important to note that the absorption feature at 107 eV is not evident in OPAL calculations for plasma temperatures lower than ~ 20 eV.

The experiments indicate that the spectral features predicted by the new opacity calculations of Rogers and Iglesias have indeed been observed. The broad nature of these $\Delta n = 0$ features is dominant in this spectral region for a wide range of plasma conditions, e.g., 10 eV with density of 10^{-5} g/cm^3 and 40 eV with density 10^{-2} g/cm^3. This is substantiated in the experiment by the existence of this absorption feature within the 1–3-ns interval recorded by the streak camera. The calculations, however, do predict that the shape, both overall strength and width, of the $\Delta n = 0$ features are sensitive to temperature. Some of the discrepancy between calculations and experiments can be attributed to the small temperature gradients present in the sample.

Finally, note that the main purpose of opacity calculations is to allow the study of radiation transport in plasmas under various conditions of temperature and density. In the present case we have provided a validation of new opacity predictions and now the much more demanding process of determining the *absolute* spectral accuracy of both experiments and predictions is appropriate.

We would like to thank the following individuals for assistance during this series of experiments: S. Mrowka, J. Kilkenny, D. Matthews, R. Wing, J. Cox, J. Koch, M. J. Edwards, and B. Stewart. This work was performed under the auspices of the U.S. Department of Energy by Lawrence Livermore National Laboratory under Contract No. W-7405-Eng-48.

[1] U. Feldman, W. E. Behring, E. L. Cohen, and G. A. Doschek, Astrophys. J. **203**, 521 (1976), for a discussion of open M-shell emission spectra.

[2] J. Reader *et al.*, J. Opt. Soc. Am. B **4**, 1821 (1987), for a discussion of $\Delta n = 0$ spectra.

[3] See, for example, A. N. Cox, Astrophys. J. **381**, L71 (1991); P. Moskalik, J. R. Buchler, and A. Marom, Astrophys. J. **385**, 685 (1992); G. Kovacs, J. R. Buchler, and A. Marom, Astron. Astrophys. **252**, L27, (1991).

[4] N. R. Simon, Astrophys. J. **260**, L87 (1982).

[5] For a summary of the Los Alamos results since 1977, see A. Weiss, J. J. Keady, and H. H. Magee, At. Data Nucl. Data Tables **45**, 209 (1990); A. N. Cox and J. E. Tabor, Astrophys. J. Suppl. Ser. **31**, 271 (1976).

[6] N. H. Magee, A. L. Merts, and W. F. Huebner, Astrophys. J. **283**, 264 (1984).

[7] G. K. Andreasen, Astron. Astrophys. **201**, 72 (1988); G. K. Andreasen and J. O. Petersen, Astron. Astrophys. **192**, 14 (1988).

[8] B. A. Remington, S. W. Haan, S. G. Glendinning, J. D. Kilkenny, D. H. Munro, and R. J. Wallace, Phys. Rev. Lett. **67**, 3259 (1991); Phys. Fluids B (to be published); J. Edwards, V. Barrow, O. Willi, and S. J. Rose, Europhys. Lett. **11**, 631 (1991).

[9] F. J. Rogers and C. A. Iglesias, Astrophys. J. Suppl. Ser. **79**, 507 (1992), and references therein.

[10] R. D. Cowan, *The Theory of Atomic Structure* (Univ. of California Press, Berkeley, 1981).

[11] D. Mihalas, *Stellar Atmospheres* (Freeman, San Francisco, 1978).

[12] R. B. Stothers and C. W. Chin, Astrophys. J. **381**, L67 (1991).

[13] D. B. Guenther *et al.*, Astrophys. J. **387**, 372 (1990).

[14] B. A. Hammel *et al.*, in *Proceedings of the 1991 Radiative Properties of Hot Dense Matter Workshop, 22*, edited by W. H. Goldstein *et al.* (World Scientific, Singapore, 1992); T. S. Perry *et al.*, Phys. Rev. Lett. **67**, 3784 (1991).

[15] D. R. Kania *et al.* (to be published); B. A. Hammel, D. R. Kania, R. Doyas, R. W. Lee, and C. A. Iglesias, Bull. Am. Phys. Soc. **36**, 2416 (1991).

[16] T. Kita, T. Harada, N. Nakana, and H. Kurada, Appl. Opt. **22**, 512 (1983); G. P. Kiehn, O. Willi, A. R. Damerell, and M. H. Key, Appl. Opt. **26**, 425 (1987).

[17] J. Edelstein, M. C. Hettrick, S. Mrowka, P. Jelinsky, and C. Martin, Appl. Opt. **23**, 3267 (1984).

[18] J. Koch and B. J. MacGowan, J. Appl. Phys. **69**, 6935 (1991).

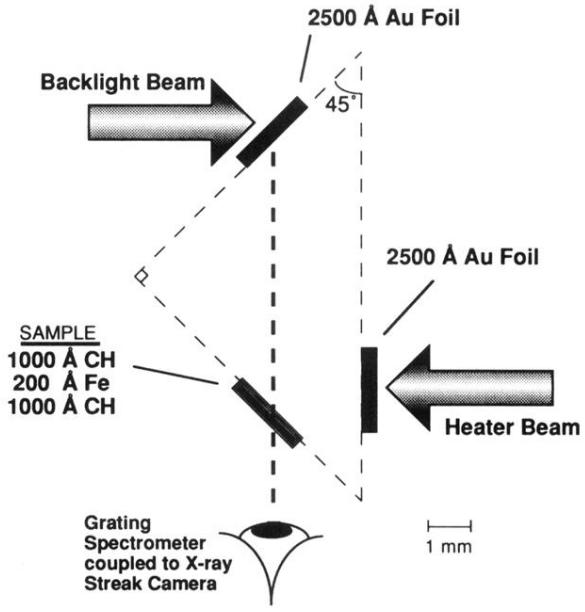

FIG. 2. A schematic drawing of the experimental setup. A laser beam irradiates a thin gold foil and produces x rays which heat the sample to be studied. Another laser beam irradiates a second gold foil over a variable 2-ns interval producing x rays which propagate through the sample and are recorded by a time-resolved grating spectrometer.

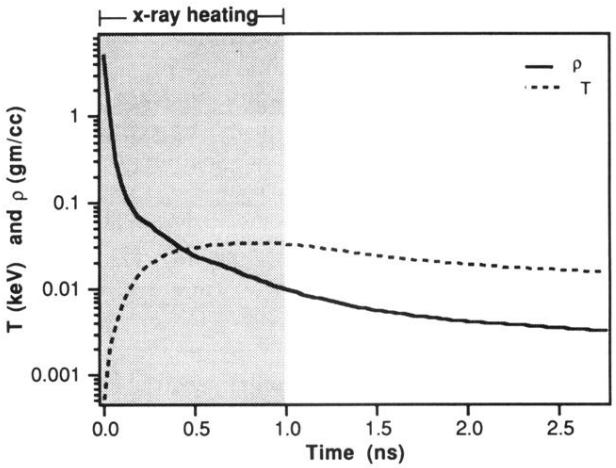

FIG. 3. Simulation of the sample under the influence of the measured x-ray flux from the heater. The temperature and the density are shown for the middle of the Fe sample vs time. The shaded region indicates the duration of the primary optical laser pulse.